

Microscopic Explanation of the Non-Arrhenius Conductivity in Glassy Fast Ionic Conductors

Philipp Maass,¹ Martin Meyer,^{2,3} Armin Bunde,² and Wolfgang Dieterich¹

¹Fakultät für Physik, Universität Konstanz, 78434 Konstanz, Germany

²Institut für Theoretische Physik III, Justus-Liebig Universität Giessen, 35392 Giessen, Germany

³Sonderforschungsbereich 173, Universität Hannover, 30176 Hannover, Germany

(Received 26 April 1996)

To explore the origin of the recently discovered non-Arrhenius behavior of the dc conductivity in glassy fast ionic conductors at high temperatures, we investigate by Monte Carlo simulations the transport of charged particles in an energetically disordered structure. We show that the combined effect of Coulomb interaction and disorder can account for the experimental findings. Our results suggest that glassy superionic conductors can be optimized by lowering the strength of the energetic disorder but that the ionic interaction effects set an upper bound for the conductivity at high temperatures. [S0031-9007(96)00980-5]

PACS numbers: 66.30.Dn, 66.30.Hs

Recently, Kincs and Martin [1] made the important discovery that the dc conductivity σ_{dc} in glassy fast ion conductors does not follow a simple Arrhenius law below the glass transition temperature. Rather, they found that the high-temperature values of σ_{dc} can be significantly smaller than expected when extrapolating the Arrhenius law valid at low temperatures T . Formally, the deviation from the Arrhenius law can be described by a temperature dependent (apparent) activation energy $E(T)$, which decreases with increasing T .

Very recently Ngai and Rizos suggested an explanation of the non-Arrhenius behavior based on the coupling concept [2] that has been proven to be a very successful phenomenological approach to describe dynamic processes in complex systems [3]. Within the coupling concept, the variation of $E(T)$ is interpreted as a crossover from a high value E_a at low T , where the conductivity relaxation is dominated by a Kohlrausch-Williams-Watts (KWW) behavior, to a smaller value E_0 at high T , where it is dominated by an exponential relaxation function.

From a microscopic point of view, a theoretical understanding of the ion transport in glasses is difficult to obtain, because only limited information is available about the detailed microscopic structure of ionic glasses [4]. The ions encounter a very complex energy landscape, whose irregularities are determined both by the random electric fields produced by the immobile counterions [5] and the spatial fluctuations in the local glass structure [6]. The Coulomb interaction between the mobile ions presents an additional difficulty for a theoretical treatment [7]. By a spatial coarse graining, one may describe the ionic motion within a simplified model [8], where only the Coulomb interaction between the mobile ions and the disorder of the glassy substrate is taken into account.

In this Letter we show explicitly that the non-Arrhenius behavior can be understood from a model of charged particles moving between the sites of a lattice with random site energies. We find that both ingredients, disorder and Coulomb interactions, are essential for describing the

experimental situation properly: At low temperatures, the conductivity shows an Arrhenius behavior (see Fig. 1),

$$\sigma_{dc}T = A_{\sigma} \exp(-E_a/k_B T), \quad (1)$$

where the activation energy E_a is determined by the combined effect of energetic disorder and interaction, whereas at high temperatures the bare interaction effects become dominant and provide an upper bound for the conductivity. Because of the existence of this bound, the conductivity fails to reach the high values expected from extrapolating its low-temperature behavior [Eq. (1)], thus giving rise to the observed non-Arrhenius behavior. Our results also account for a further feature of the Kincs and Martin discovery: The deviation from the Arrhenius law already occurs at temperatures where the thermal energy $k_B T$ is by more than 1 order of magnitude smaller than the low-temperature activation energy E_a (see Fig. 1).

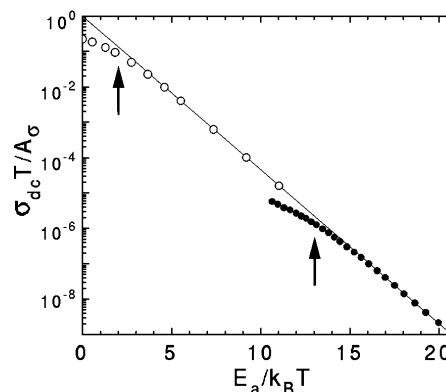


FIG. 1. Arrhenius plot of $\sigma_{dc}T$ for $c = 0.01$ when neglecting the Coulomb interaction (open symbols), and for $0.4\text{AgI} + (0.6)[0.525\text{Ag}_2\text{S} + 0.475(\text{B}_2\text{S}_3:\text{SiS}_2)]$ (filled symbols, redrawn from 1). In both cases $\sigma_{dc}T$ has been normalized with respect to the preexponential factor A_{σ} of the low-temperature Arrhenius law, and the activation energy E_a has been used to scale the temperature. The arrows indicate the crossover points, where the Arrhenius law ceases to be valid. The solid line is drawn as a guide for the eye.

To model the ion dynamics, we choose a simple cubic lattice with lattice spacing ξ , where ξ is the typical distance over which the energies along the ionic diffusion pathways are correlated. To each lattice site i we assign an energy ϵ_i drawn from a Gaussian distribution $P(\epsilon)$ with zero mean and variance σ_ϵ^2 . The number of mobile ions per lattice site is $c \ll 1$ and $\rho = c/\xi^3$ denotes the ionic number density.

First we neglect the long range Coulomb interaction. Assuming that sites cannot be occupied by more than one ion, the ions in equilibrium are distributed according to a Fermi distribution. The ions hop among nearest neighbor sites and the jump rate from site i to a vacant site j is given by $W_{ij} = \nu \min(1, \exp[-(\epsilon_j - \epsilon_i)/k_B T])$, where ν is an attempt frequency [9]. Similar models of noninteracting particles in a disordered energy landscape have been studied earlier [10,11], and mainly focused on a theoretical description of the conductivity dispersion below the GHz regime. At low temperatures $T \ll \sigma_\epsilon/k_B$, the activation energy can be calculated according to a critical path argument [12,13], $E_a = \epsilon_c - \epsilon_f(c)$. Here $\epsilon_f(c)$ is the Fermi energy, defined by $\int_{-\infty}^{\epsilon_f} P(\epsilon) d\epsilon = c$, and ϵ_c is given by $\int_{-\infty}^{\epsilon_c} P(\epsilon) d\epsilon = p_c$, where p_c is the percolation threshold [14] in the sc lattice, $p_c \approx 0.3117$. For a typical concentration $c = 0.01$ we obtain $E_a = 1.84\sigma_\epsilon$. Because of the very weak dependence of ϵ_f on c , E_a assumes similar values for any reasonable concentration $c \ll 1$.

At high temperatures $T \gg \sigma_\epsilon/k_B$, the conductivity is well approximated by $\sigma_{dc} \approx \rho q^2 \xi^2 \langle W \rangle / 6k_B T$, where q is the charge of the mobile ions and $\langle W \rangle$ the mean jump rate. As can be shown by a high-temperature expansion, $\langle W \rangle$ is given by $\langle W \rangle \approx (1 - c)(1 - \sigma_\epsilon/\sqrt{\pi} k_B T) \approx (1 - c) \exp(-\sigma_\epsilon/\sqrt{\pi} k_B T)$, in leading order of $\sigma_\epsilon/k_B T$. Hence we obtain a high-temperature activation energy $E_0 = \sigma_\epsilon/\sqrt{\pi} \approx 0.56\sigma_\epsilon$ that is smaller than E_a . Accordingly, $E(T)$ changes from E_a for low temperatures to E_0 at a crossover temperature $T_x \approx \sigma_\epsilon/k_B$. Notice that both E_a and $k_B T_x$ are of the same order of magnitude, determined by σ_ϵ , which disagrees with the experimental result that the non-Arrhenius behavior sets in at temperatures more than 1 order of magnitude smaller than E_a/k_B .

This can be seen clearly in Fig. 1, where we compare the temperature dependence of σ_{dc} in the absence of Coulomb interactions with the experimental results of Kincs and Martin [1]. The filled circles are the experimental data. The open circles are from Monte Carlo simulations (see below) for $c = 0.01$, and are in perfect agreement with the theoretical predictions discussed above. The arrows indicate the crossover temperatures and show that both disagree by about an order of magnitude.

Next we include the Coulomb interaction. Since an analytic treatment is no longer possible, we study the model by computer simulations. We performed Monte Carlo simulations in a sc lattice of size $L = 40\xi$ with

periodic boundary conditions for a fixed ionic concentration $c = 0.01$. The Coulomb energies were calculated by the Ewald method [15] and the standard Metropolis algorithm was used to simulate the hopping dynamics [16]. (For a more detailed description of the simulation technique see [8].) We choose $V_c \equiv q^2/R$ as the energy unit, where $R \equiv (3/4\pi\rho)^{1/3}$ is the half mean distance between the mobile ions. It is reasonable to assume that glassy fast ionic conductors have similar values V_c , because their ionic concentrations and high-frequency dielectric constants do not vary drastically [17]. We investigate the behavior of the tracer diffusion coefficient D as a function of the reduced temperature and the strength of the disorder σ_ϵ . The diffusion coefficient D was determined from the long time limit of the mean square displacement $\langle r^2(t) \rangle$ of a tracer ion, $D = \lim_{t \rightarrow \infty} \langle r^2(t) \rangle / 6t$. As was shown earlier [8], σ_{dc} is, in a good approximation, related to D via the Nernst-Einstein relation, $\sigma_{dc} = \rho q^2 D / k_B T$ [18].

Figure 2(a) shows the normalized diffusion coefficient D/D_0 ($D_0 \equiv \nu \xi^2 / 6$) as a function of $V_c/k_B T$ for various disorder strengths $\sigma_\epsilon/V_c = 0.0115, 0.018, 0.036, \text{ and } 0.072$. At low temperatures, each curve follows a straight line corresponding to an Arrhenius law with constant activation energy E_a , and E_a decreases with decreasing σ_ϵ . The Arrhenius law is valid up to a crossover temperature T_x , where the curves bend toward lower diffusivities. In all cases, the crossover temperature T_x is of the order of σ_ϵ/k_B . For comparison we have redrawn in Fig. 2(b) the experimental conductivity data for $z\text{AgI} + (1 - z)[0.525\text{Ag}_2\text{S} + 0.475(\text{B}_2\text{S}_3:\text{SiS}_2)]$ with mole fractions z between zero and 0.4 [1] (note that $D \sim T\sigma_{dc}$). Evidently, when increasing z , the experimental behavior is analogous to the model behavior when decreasing σ_ϵ : E_a becomes smaller and the non-Arrhenius behavior starts to occur at lower T .

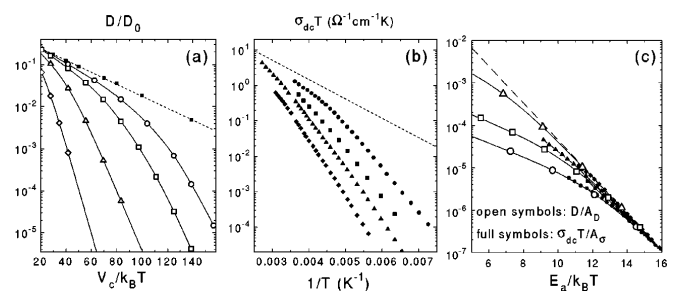


FIG. 2. Arrhenius plots of (a) the normalized diffusion coefficient D/D_0 in the model for $\sigma_\epsilon/V_c = 0$ (\blacksquare), 0.0115 (\circ), 0.018 (\square), 0.036 (\triangle), and 0.072 (\diamond), and (b) the conductivity in $z\text{AgI} + (1 - z)[0.525\text{Ag}_2\text{S} + 0.475(\text{B}_2\text{S}_3:\text{SiS}_2)]$ for $z = 0$ (\blacklozenge), 0.2 (\blacktriangle), 0.3 (\blacksquare), and 0.4 (\bullet) (redrawn from 1). The dashed lines indicate the upper mobility limit predicted by the model. In (c) the data from (a) and (b) are shown together as functions of $E_a/k_B T$ and are normalized with respect to the preexponential factors A_D and A_σ in the corresponding Arrhenius laws. The solid lines in (a) and (c) are drawn as a guide for the eye.

The similarity between the results found in the model and in the experiment becomes even more evident in Fig. 2(c), where the data from Figs. 2(a) and 2(b) are plotted in the same way as in Fig. 1. The experimental curve for $z = 0.4$ is almost perfectly reproduced by the model when $\sigma_\epsilon = 0.0115V_c$ [see the filled and open circles in Fig. 2(c)]. The experimental curves for $z = 0, 0.2,$ and 0.3 correspond to disorder strengths within a range $0.015V_c < \sigma_\epsilon < 0.036V_c$. It is remarkable that the model not only gives a good fit to the overall shape of the conductivity curves but also reproduces the small values of $k_B T_x / E_a$.

In order to understand why $k_B T_x / E_a$ becomes much smaller than one for small σ_ϵ , we need to know how E_a depends on σ_ϵ quantitatively. We therefore plotted in Fig. 3 E_a / V_c (resulting from our computer simulations) as a function of σ_ϵ / V_c and find that E_a / V_c increases linearly with σ_ϵ / V_c ,

$$E_a = a_1 V_c + a_2 \sigma_\epsilon, \quad (2)$$

where $a_1 = 0.10$ and $a_2 = 1.84$ for $c = 0.01$. Since $T_x \approx \sigma_\epsilon / k_B$, we obtain $k_B T_x / E_a \approx \sigma_\epsilon / (a_1 V_c + a_2 \sigma_\epsilon) \sim \sigma_\epsilon / a_1 V_c$ for $\sigma_\epsilon \rightarrow 0$, and accordingly $k_B T_x / E_a$ becomes much smaller than one for small σ_ϵ . We note that for large $\sigma_\epsilon \gg V_c$, $E_a \approx a_2 \sigma_\epsilon$, which agrees with the result $E_a = 1.84 \sigma_\epsilon$ for $\sigma_\epsilon / V_c \rightarrow \infty$, i.e., in the disordered system without Coulomb interaction (see the critical path analysis given above). However, when extrapolating Eq. (2) to $\sigma_\epsilon = 0$, we obtain $E_a = 0.10 V_c$, which is more than 3 times larger than the value $E_a^{(0)} = 0.032 V_c$ in the ordered system (see the dashed and dotted lines in Fig. 3). This is an interesting disorder effect: The constant activation energy E_a is reached at temperatures $T \ll T_x \approx \sigma_\epsilon / k_B$, and in this regime even arbitrary small energy fluctuations seem to increase the activation energy by a factor of about 3.

Based on the success of the model, we are now able to discuss the origin of the non-Arrhenius behavior and the associated problem of optimized ionic conduction.

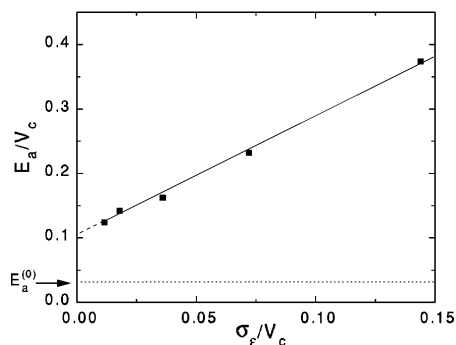


FIG. 3. Simulated activation energy E_a / V_c as a function of the strength of the disorder σ_ϵ / V_c . The dotted line indicates the activation energy $E_a^{(0)}$ in the ordered system ($\sigma_\epsilon = 0$), which is about 3 times smaller than the limiting value for $\sigma_\epsilon \rightarrow 0$.

The non-Arrhenius behavior occurs as a result of a crossover between two different temperature regimes: For $T \ll T_x$, the activation energy E_a is governed by the combined effect of the energetic disorder and the Coulomb repulsion between the mobile ions [as shown in Eq. (2)], while for $T \gg T_x$ the apparent activation energy becomes smaller, because the disorder becomes irrelevant and the ionic mobility is governed by the effects of the Coulomb interaction alone [19]. Accordingly, for $T \gg T_x$ all curves in Fig. 2(a) approach the dashed line with slope $E_a^{(0)} / V_c$, which corresponds to the values obtained in the ordered system. The dashed line thus sets an upper bound for the ionic mobility, which by reducing σ_ϵ is approached at lower temperatures. This way the conductivity is optimized by extending the high-temperature regime to lower temperatures, i.e., by decreasing T_x .

The analogous behavior occurs in the experiment when z is increased [see Fig. 2(b)], which suggests that the disorder of the ionic pathways is decreased by increasing the iodine content. (This does, however, not necessarily imply that the iodine ions form some regularly structured α -AgI-like microdomains in the glassy network, as it was conjectured, e.g., in [20] but later questioned in [21].) One can roughly estimate the location of the experimental limiting curve by extrapolating the conductivity data in Fig. 2(b) to higher temperatures. The resulting curve is drawn as dashed line in Fig. 2(b) and has an activation energy $E_0 = 0.11$ eV. In order to check for consistency, we compare this value with the activation energy $E_a^{(0)} = 0.032 V_c$ of the limiting curve in the model. As a result we get $V_c = 3.4$ eV, which is an acceptable value. For example, if we assume that the number density of Ag^+ ions is about $2 \times 10^{22} \text{ cm}^{-3}$ as in $z\text{AgI} + (1 - z)\text{Ag}_2\text{O-B}_2\text{O}_3$ [22], and that the high-frequency dielectric constant is $\epsilon_\infty \approx 2$, we obtain $V_c \approx 3.3$ eV.

In summary, we have studied the transport of ions in an energetically disordered structure and found that in the presence of both disorder and Coulomb interaction the non-Arrhenius behavior observed in a series of glassy fast ion conductors is correctly reproduced. We have shown that by decreasing the strength of the energetic disorder, the activation energy can be systematically lowered and the crossover temperature T_x to the non-Arrhenius regime becomes smaller. According to this observation one may understand why the non-Arrhenius behavior has been found in fast ion conducting glasses and is commonly not observed in traditional ionic glasses, as, e.g., $\text{Na}_2\text{O-3SiO}_2$. In these traditional ionic glasses the activation energies are relatively large and one would thus expect that the strength of the energetic disorder is also large. As a consequence, the crossover temperature should be high and might not be reached below the glass transition.

Moreover, one may understand why the non-Arrhenius behavior for certain other fast ion conducting glasses can

be removed by annealing [23]. After the annealing process the glass belongs to a lower fictive temperature; i.e., its structure has become more heterogeneous and more dissimilar with respect to that in the melt. Accordingly, the energetic disorder should be larger and the crossover temperature to the non-Arrhenius behavior could have been shifted beyond the glass transition temperature. This reasoning can easily be tested by choosing smaller “annealing steps,” which would allow one to follow the change in the crossover temperature systematically.

We thank M.D. Ingram and P. Pendzig for very valuable discussions and acknowledge financial support from the Deutsche Forschungsgemeinschaft (SFB 173 and 306).

-
- [1] J. Kinsc and S. W. Martin, Phys. Rev. Lett. **76**, 70 (1996).
 [2] K. Ngai and A. K. Rizos, Phys. Rev. Lett. **76**, 1296 (1996).
 [3] K. L. Ngai, Comments Solid State Phys. **9**, 127 (1979); **9**, 141 (1979).
 [4] M. D. Ingram, Phys. Chem. Glasses **28**, 215 (1987).
 [5] W. Dieterich, D. Knödler, and P. Pendzig, J. Non-Cryst. Solids **172–174**, 1237 (1994).
 [6] P. Maass, A. Bunde, and M. D. Ingram, Phys. Rev. Lett. **68**, 3064 (1992); A. Bunde, M. D. Ingram, and P. Maass, J. Non-Cryst. Solids **172–174**, 1222 (1994); A. Bunde, K. Funke, and M. D. Ingram, Solid State Ion. (to be published).
 [7] K. Funke, Z. Phys. Chem. Neue Folge **154**, 251 (1987); K. Funke, Prog. Solid State Chem. **22**, 111 (1993).
 [8] P. Maass, J. Petersen, A. Bunde, W. Dieterich, and H. E. Roman, Phys. Rev. Lett. **66**, 52 (1991); M. Meyer, P. Maass, and A. Bunde, Phys. Rev. Lett. **71**, 573 (1993).
 [9] The spatial coarse graining on a length scale ξ represents an approximate procedure, which allows one to study the low-frequency dynamics. The attempt frequency is chosen as $\nu \equiv v_{th}^2/\gamma\xi^2$, where $v_{th} = (k_B T/m)^{1/2}$ is the thermal velocity and γ the friction constant.
 [10] W. Schirmacher, M. Prem, J.-B. Suck, and A. Heidemann, Europhys. Lett. **13**, 523 (1990).
 [11] J. C. Dyre, Phys. Rev. B **48**, 12511 (1993).
 [12] V. Ambegoakar, B. I. Halperin, and J. S. Langer, Phys. Rev. B **4**, 2612 (1971); B. I. Shklovskii and A. L. Efros, Zh. Eksp. Teor. Fiz. **60**, 867 (1971) [Sov. Phys. JETP **33**, 468 (1971)].
 [13] H. Bässler, Phys. Rev. Lett. **58**, 767 (1987).
 [14] A. Bunde and S. Havlin, in *Fractals and Disordered Systems*, edited by A. Bunde and S. Havlin (Springer, Heidelberg, 1996), 2nd ed.
 [15] M. P. Allen and D. J. Tildesley, *Computer Simulation of Liquids* (Clarendon, Oxford, 1987).
 [16] K. Binder and D. W. Heermann, *Monte Carlo Simulations in Statistical Physics*, Springer Series in Solid State Science Vol. 80 (Springer, Berlin, Heidelberg, 1992), 2nd ed.
 [17] We note that the Coulomb interaction $V_c = q^2/R$ in the model already contains the high-frequency dielectric constant ϵ_∞ in the glass, i.e., $V_c = e^2/\epsilon_\infty R$.
 [18] The Haven ratio $H_R \equiv \sigma_{dc} k_B T / \rho q^2 D$, which quantifies the contribution from the cross terms in the current correlation function, is almost independent of temperature and varies from about 0.4 to almost 1 if σ_ϵ is increased. Similiar values are generally found in the experiments [4].
 [19] One can estimate that below reasonable calorimetric glass transition temperatures the thermal energy $k_B T$ will not exceed the characteristic Coulomb energy V_c , i.e., the Coulomb interaction cannot be neglected (with the exception of very dilute systems).
 [20] M. Tachez, R. Mercier, J. P. Malugani, and A. J. Dianoux, Solid State Ion. **20**, 93 (1986).
 [21] L. Börjesson, L. M. Torell, and S. W. Howells, Philos. Mag. B **59**, 105 (1989).
 [22] T. Minami, T. Shimizu, and M. Tanaka, Solid State Ion. **9 & 10**, 577 (1983).
 [23] M. D. Ingram, C. Vincent, and A. Wandless, J. Non-Cryst. Solids **53**, 73 (1982).